

Supplementary Information

for

**Derivation of Moisture-Driven Landslide Thresholds for
Northeastern Regions of the Indian Himalayas**

Danish Monga¹, Poulomi Ganguli^{1*}

¹Agricultural and Food engineering department, Indian Institute of Technology Kharagpur,
Kharagpur India

**Correspondence to:* Poulomi Ganguli (pganguli@agfe.iitkgp.ac.in)

Contents of this file

Figures S1 to S7

Tables S1

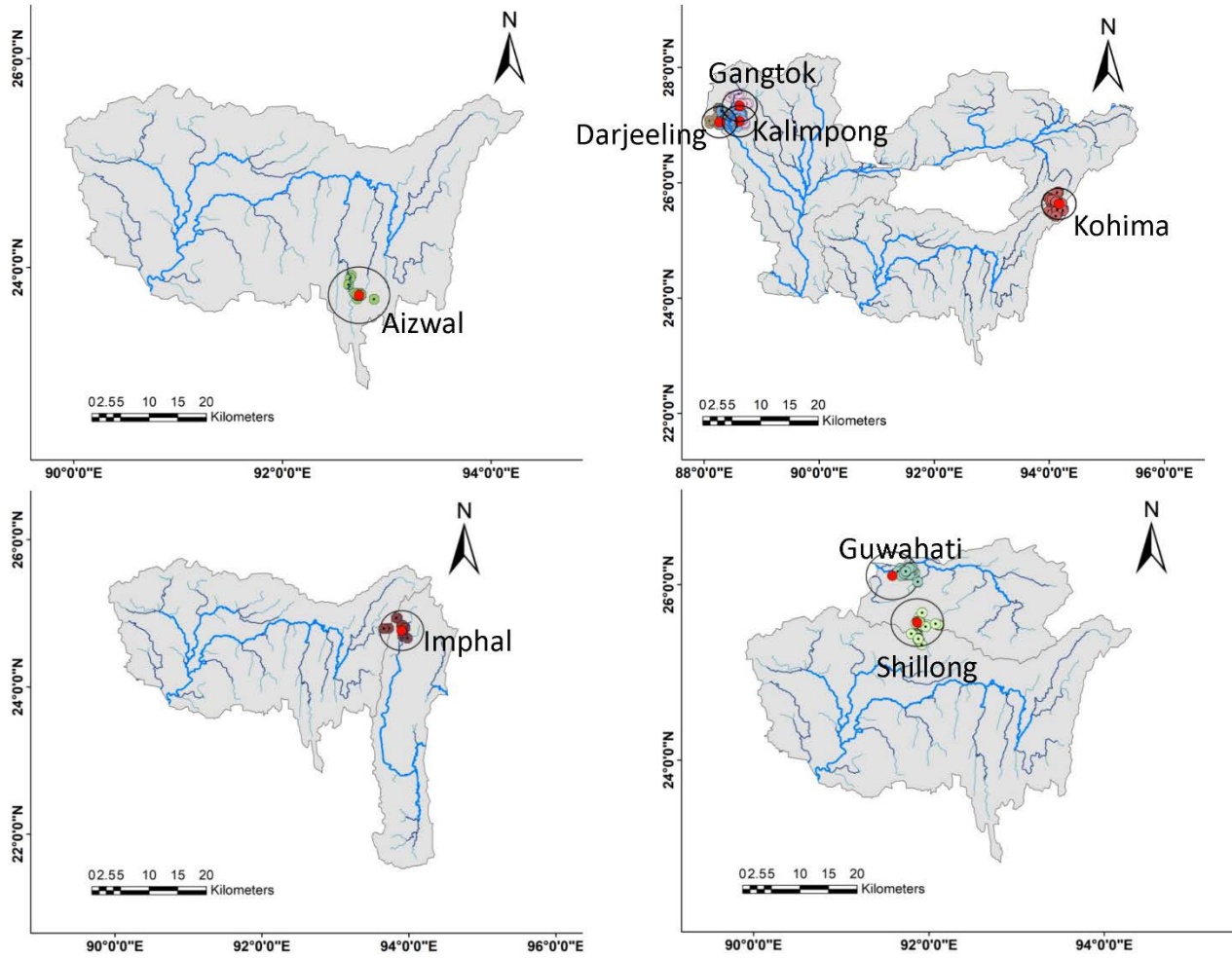


Figure S1: Sub-catchments and hydrometric observatories in NE Himalayas. The circles show landslide inventories within 30 km radius (2007–2019).

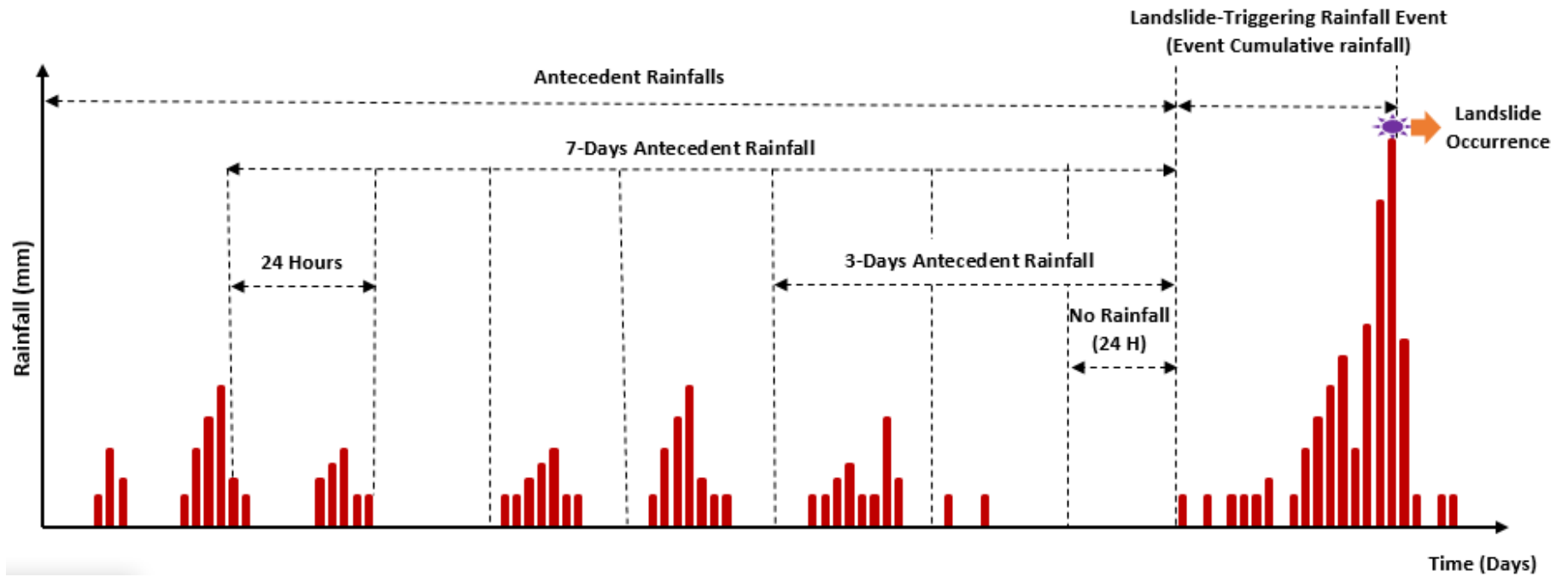


Figure S2: Schematic representation of antecedent versus triggering rainfall events, illustrating cumulative antecedent rainfall periods and the critical 24-hour no-rainfall interval before the landslide-triggering event.

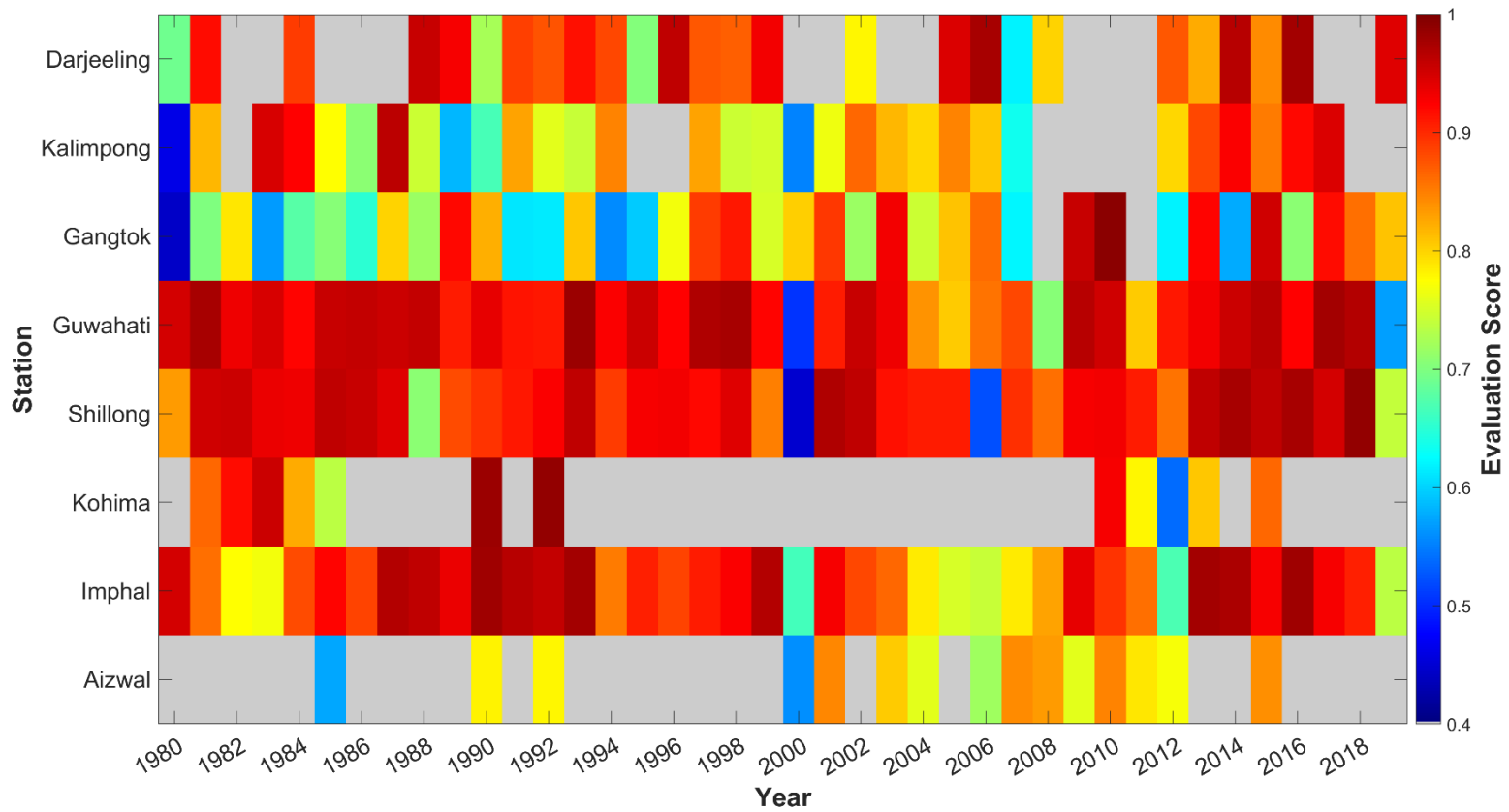


Figure S3: Efficacy of the Regularized Expectation Maximization (RegEM) method in infilling gaps of rainfall time series from 1980 to 2019. The performance scores range from excellent (0.99) to modest (0.45), with notable efficacy observed across Guwahati and Shillong, whereas the performance drops across sites and time windows with fewer observations, *e.g.*, Aizwal and Kohima.

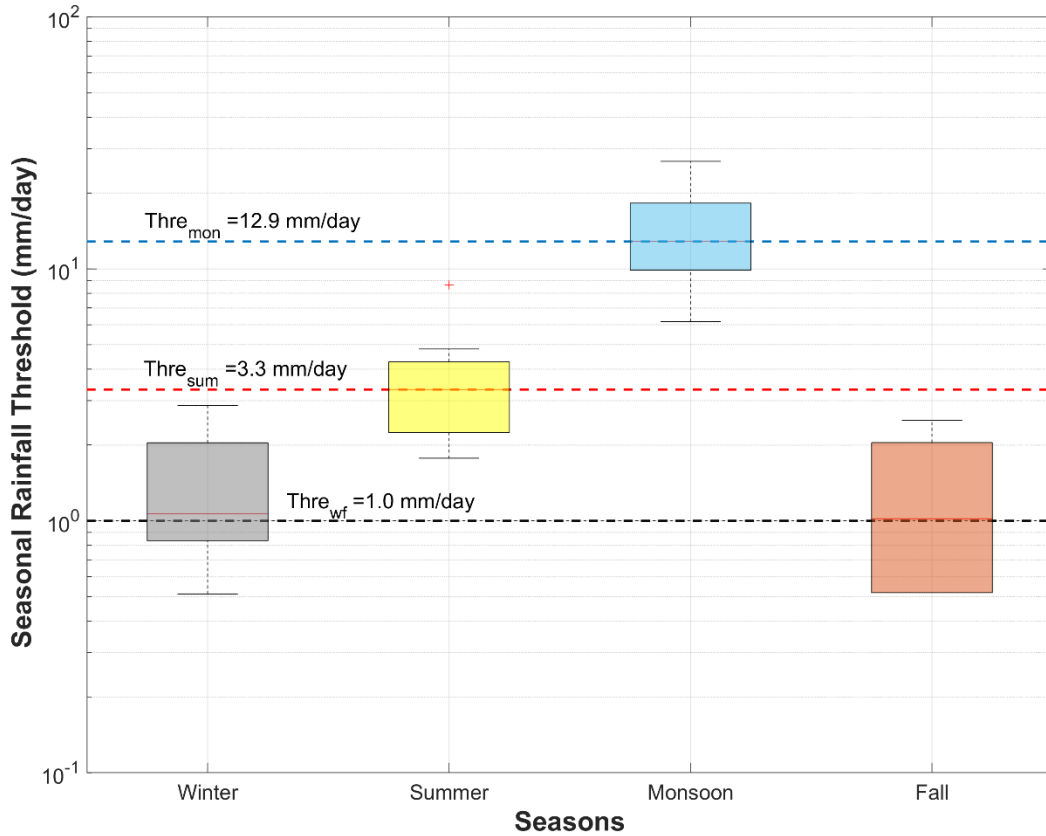


Figure S4: Box plot illustrating seasonal rainfall thresholds for detecting rain events in the NEH region. The seasonal rainfall thresholds exhibit notable variability, with the highest threshold observed during the monsoon season (July to September), ranging from 6.2 to 26.7 mm/day with a median of 12.9 mm/day (marked by the blue dashed line). In contrast, the summer season (April to June) rain threshold shows a median value of 3.3 mm/day (in red dashed line), while both the fall (October to December) and winter (January to March) seasons have relatively lower median thresholds of 1.0 mm/day each (shown in black dashed line).

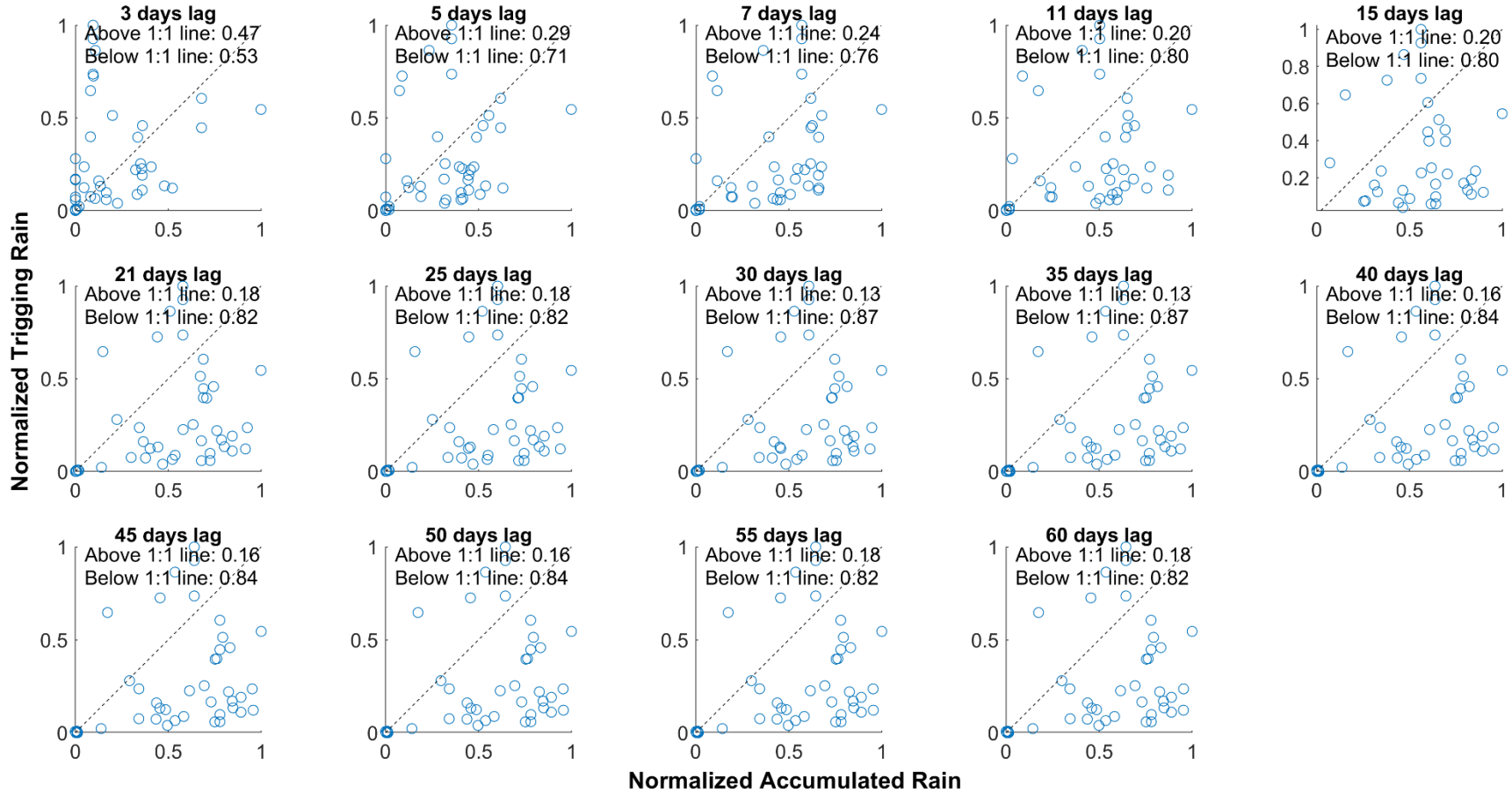


Figure S5: Scatter plots of normalized cumulative rainfall versus normalized triggering rain events at different time lags (3 to 60 days) for Gangtok. Scattering bias increases with longer time lags, as observed with the 3-day lag showing 47% of triggering events above the 1:1 line, whereas at 60-day lag the scattering bias drops to 18%. Both the 30-day and 35-day lags show 87% of events below the 1:1 line. Finally, the 35-day time lag is chosen as the optimal considering the robust correlation (Kendall's $\tau \approx 0.31$ with a p-value < 0.05) between antecedent vs triggering rain events.

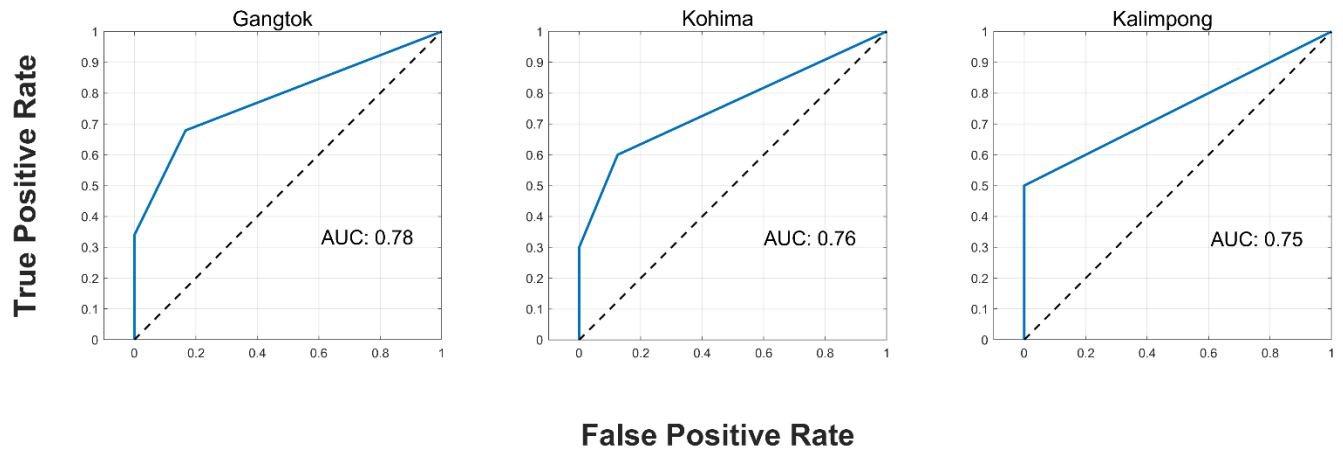


Figure S6: Performance assessments of developed rain threshold models for MDLs across representative sites. ROC-AUC curves showing the statistical validation of the ED thresholds for landslide prediction across Gangtok, Kohima, and Kalimpong. The numbers on the plot showing the AUC values demonstrates strong predictive capability of the derived model.

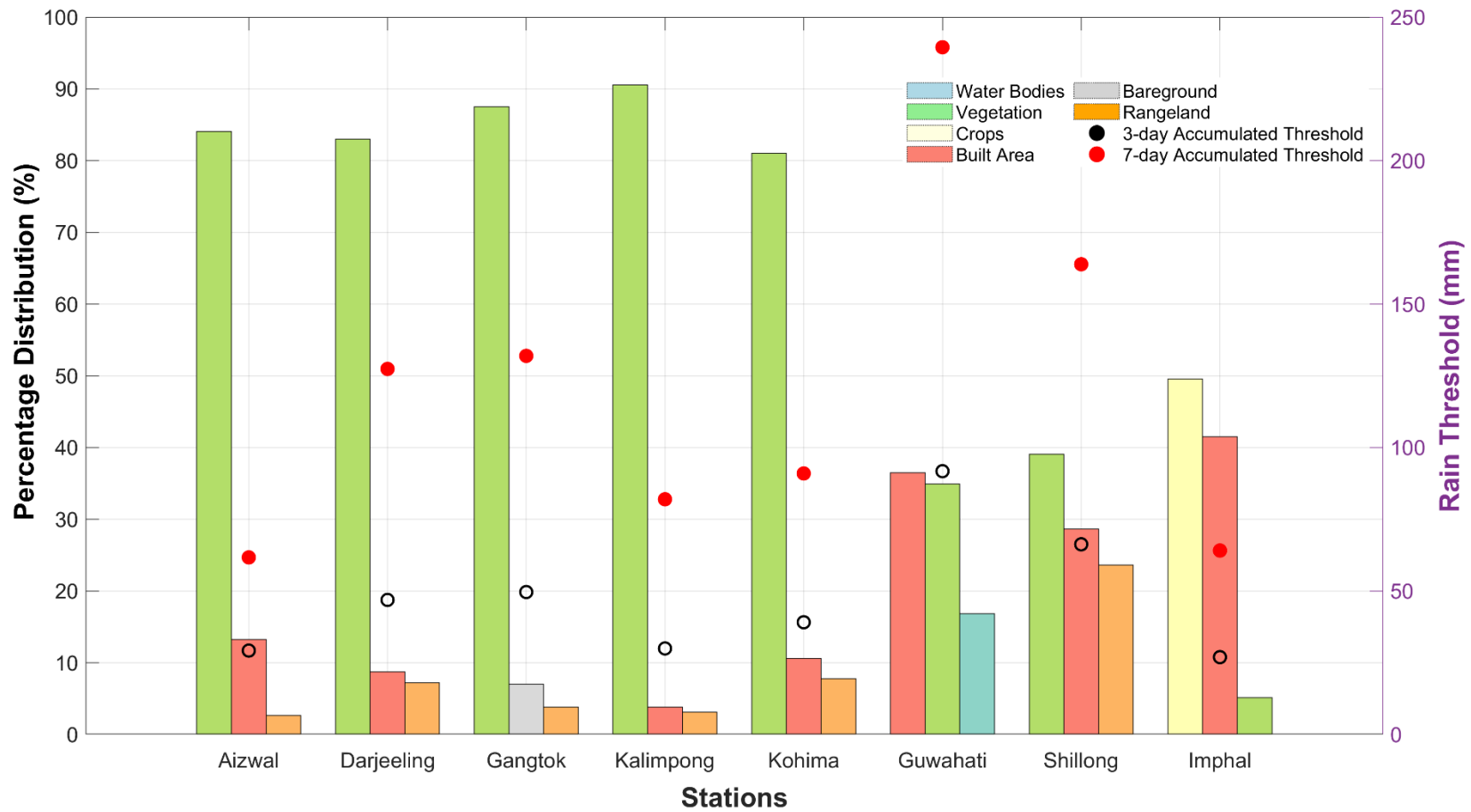


Figure S7: Assessment of top three land use/land cover classes and their rainfall thresholds across NERI locations highlighting significant variability in rainfall thresholds for MDLs. The spatial variability (shown using %), depicted by open (sub-weekly time scale) and filled (weekly time scale) circles highlights LULC controls on rain thresholds for landslide trigger.

Table S1: Intercept and slope values for at-site ED thresholds derived from the 20th percentile accumulated rainfall-duration relationship.

WMO ID	Name	Parameters	
		Intercept (a)	Slope (b)
42295	Darjeeling	-14.0	19.20
42296	Kalimpong	-4.0	7.0
42299	Gangtok	-13.20	16.93
42410	Guwahati	-0.23	15.82
42516	Shillong	-10.0	23.40
42527	Kohima	4.16	8.04
42623	Imphal	-2.20	6.0
42727	Aizwal	3.80	8.30